ISSN (Print) 1226-1750
ISSN (Online) 2233-6656
Journal of Magnetics 25(2), 133-139 (2020) https://doi.org/10.4283/JMAG.2020.25.2.133

Preparation and Characterization of Magnesium Zinc Ferrite Barium Strontium Titanate Composite Materials using Two Stage Sintering

A. Sutthapintu and A. Rittidech*

Department of Physics, Faculty of Science Mahasarakham University, Mahasarakham 44150, Thailand

(Received 4 February 2020, Received in final form 10 June 2020, Accepted 18 June 2020)

The effect of two-stage sintering of composition ceramics between (0.6)$Mg_{0.7}Zn_{0.3}Fe_2O_4$ and (0.4)$Ba_{0.7}Sr_{0.3}TiO_3$ on crystal structure, microstructure, electrical and magnetic properties was studied. Samples were sintered using a two-stage sintering method with the first sintering temperature (T_1) at 1350 ºC with different holding times for 30, 50 and 60 min and cooled down to the second sintering temperature (T_2) with sintering temperatures at 900 °C and 1100 ºC for 5 h with heating/cooling rate at 10 ºC/min. It was found that the densities and shrinkage values tended to slightly increase with the length of holding times at T_1. XRD patterns showed a combination phase between $Mg_{0.7}Zn_{0.3}Fe_2O_4$ and $Ba_{0.7}Sr_{0.3}TiO_3$. The crystallize size and lattice strain were calculated from XRD patterns and found to increase with T_2 sintering. EDX analysis was used to confirm the elemental composition percentage of (0.6)MZF-(0.4)BST. Examination of the microstructure of composition ceramics with SEM revealed grain sizes in the range of 0.852-1.877 μm; with, square shaped grains corresponding to the $Mg_{0.7}Zn_{0.3}Fe_2O_4$ phase and round oval shape corresponding with $Ba_{0.7}Sr_{0.3}TiO_3$ phase. Magnetic behavior and dielectric constant are obviously increased with highly dense ceramics. Finally, the optimal conditions of two stage sintering were obtained for the holding times of T_1 about 50-60 min and the second sintering temperature of T_2 at 900 °C for 5 h.

Keywords : two-stage sintering, (0.6)MZF-(0.4)BST, XRD

1. Introduction

Multiferroic materials with simultaneous ferromagnetic and ferroelectric properties have attracted considerable attention in the recent years. Considerable efforts have been put into the multiferroics due to their potential uses as sensors, transducers and actuators [1-3]. In multiferroic materials, a dielectric polarization and a magnetic moment can be induced by an external magnetic field. This phenomenon is described as the magnetoelectric effect [4]. However, the properties of multiferroic materials are dependent on microstructure, densification, preparations and sintering temperature. To date, two main groups of multiferroic composite ceramics are available based on the combination of ferromagnetic and ferroelectric ceramic materials [5]. The synthesis of multiferroic materials with simultaneous ferromagnetic properties has been the focus of much research effort to study the ferromagnetic properties of $Mg_{0.7}Zn_{0.3}Fe_2O_4$ and ferroelectric properties of $Ba_{0.7}Sr_{0.3}TiO_3$ but studies have now shifted to explore multiferroic composite materials [6, 7].

Rittidech *et al*. [8] investigated the synthesis and characterization of (1-x) $Mg_{0.7}Zn_{0.3}Fe_2O_4$-(x)$Ba_{0.7}Sr_{0.3}TiO_3$ ceramic composite with x ranging from 0.0 to 1.0 using conventional sintering and they observed that the optimal magneto-electric properties were obtained from highly dense of ceramic composite by (0.6)$Mg_{0.7}Zn_{0.3}Fe_2O_4$-(0.4)$Ba_{0.7}Sr_{0.3}TiO_3$ system. Moreover, it was found that the weight loss of ceramic composite during sintering procedure is the result of sintering at high temperatures for a long time, in consistent with the densification results. The densification process is high relative to that for grain growth, sample with finer grain microstructure can be produced by high temperature, short-time firing cycles [9]. Multiferroic materials with highly dense and fine grain provide good electrical and magnetic properties that are used for application in magneto-electric devices. The cause of this phenomenon may be related with specific area, which increased with the decrease of grain size and low porosity [10]. The (0.6)$Mg_{0.7}Zn_{0.3}Fe_2O_4$-(0.4)$Ba_{0.7}Sr_{0.3}TiO_3$ system represents a good multiferroic

*Corresponding author: Tel: +66-43-754379
Fax: +66-43-754379, e-mail: aurawan.r@msu.ac.th

materials with properties between ferroelectrics and ferromagnetic. Therefor, $(0.6)Mg_{0.7}Zn_{0.3}Fe_2O_4$-$(0.4)Ba_{0.7}Sr_{0.3}TiO_3$ ceramic composite has received attention in improving the properties from the preparation process.

The properties of materials are dependent on several factors including the sintering temperature. Previous work [8, 11] reported that the composite ceramics of ferroelectric and ferromagnetic materials synthesized by conventional sintering are probably due to some oxide loss impending the sintering process. The occurrence of weight losses of ceramics at high sintering temperature leads to low densification values. Considerable improvement in multiferroic properties of fabricated ceramics have been observed. Some investigators were able to fabricate dense ceramics with better properties using other sintering method such as hot pressing and spark plasma sintering, instead of conventional methods [12]. The development of high-density ceramic materials has been studied to considerably improve their properties for high performance applications. Two stage sintering methodologies are known: sintering with thermal pretreatment at a high sintering temperature for short holding times, followed by a second stage at lower temperature for long holding times. In the more recent approach reported by Chen and Wang [13] the first-stage high temperature sintering step helps eliminate supercritical pores while the second-stage low temperature sintering step suppresses grain growth [14].

The aim of this research is to present the optimal condition of two state sintering influence on $(0.6)Mg_{0.7}Zn_{0.3}Fe_2O_4$-$(0.4)Ba_{0.7}Sr_{0.3}TiO_3$ ceramics properties such as crystalline structure, microstructure, magnetic and electrical properties. This two-step sintering method has been applied with great success in obtaining dense ceramics with unique fine microstructures.

2. Experimental

The $(0.6)Mg_{0.7}Zn_{0.3}Fe_2O_4$-$(0.4)Ba_{0.7}Sr_{0.3}TiO_3$: (0.6)MZF-(0.4)BST was synthesized by solid state reaction and a two-step sintering method. The starting materials were commercially available oxide powders of MgO, ZnO, Fe_2O_3, $BaCO_3$, $SrCO_2$ and TiO_2. First, MZF powder was prepared by MgO, ZnO and Fe_2O_3 ball milling for 12 h and calcined at 1100 °C for 2 h. Second, BST powder was mixed with $BaCO_3$, $SrCO_2$ and TiO_2 for 12 h and then dried in air. BST precursor powders were calcined at 1150 °C for 2 h. Finally, the (0.6)MZF-(0.4)BST powders were mixed by weight percentage. The mixed powders were pressed into disks with a diameter of 13 mm and the disks were sintered by two-step sintering conditions. The temperatures for the first step (T_1) at 1350 °C for various holding times from 30, 50 and 60 min, while the temperatures for the second step (T_2) from 900 °C (batch A1, A2 and A3) and 1100 °C (batch B1, B2 and B3). The heating rate from room temperature to T_1 was 10 °C/min. The cooling rate from T_1 to T_2 was 10 °C/min. The holding times for the second step (T_2) was 5 h. After sintering, the apparent densities of the samples were measured using the Archimedes method. Phase identification was then performed using an X-ray diffractometer (XRD; Bruker model D8 advance). Next, Rietveld refinement of the XRD patterns of all samples was carried out by TOPAS software. The micro structures were observed via scanning electron microscopy (SEM, JEOL, JSM-840A, Japan). The dielectric measurements with respect to frequency were made using an automated measurement system, i.e. an LCR meter (HP-4174A). The magnetic evaluation was carried out at room temperature using Vibrating Sample Magnetometer (In-house developed VSM).

3. Results and Discussion

The XRD pattern of (0.6)MZF-(0.4)BST ceramics sintered with different two stage sintering conditions is showed in Fig. 1. The characteristic peaks of MZF and BST structure were formed. The main refraction of spinel MZF in the pattern from planes (220), (311), (400), (511) and (440) match well with JCPDS file no. 00-008-0234 [15, 16]. Likewise, the tetragonal perovskite phase of BST could be indicated as (100), (110), (111), (002) and (211) planes and indexed to the JCPDS file no. 89-0274 [17]. The ZnO phase appeared at 2-theta about 34° and was clearly apparent in sample batch B. XRD patterns of MZF and BST composite materials show the two main phase combination similar to previous work conducted on

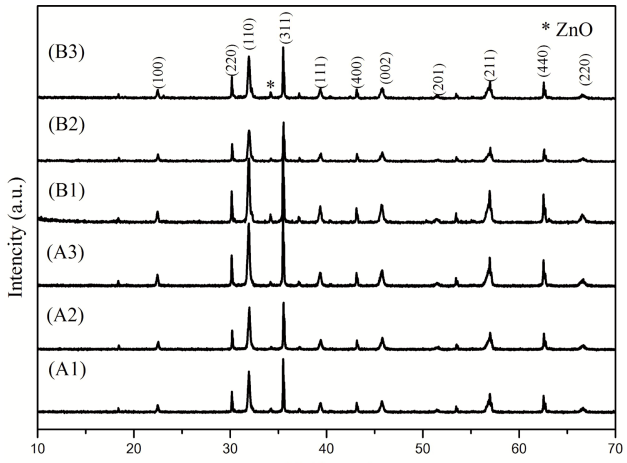

Fig. 1. XRD patterns of (0.6)MZF-(0.4)BST ceramics under two stage sintering conditions.

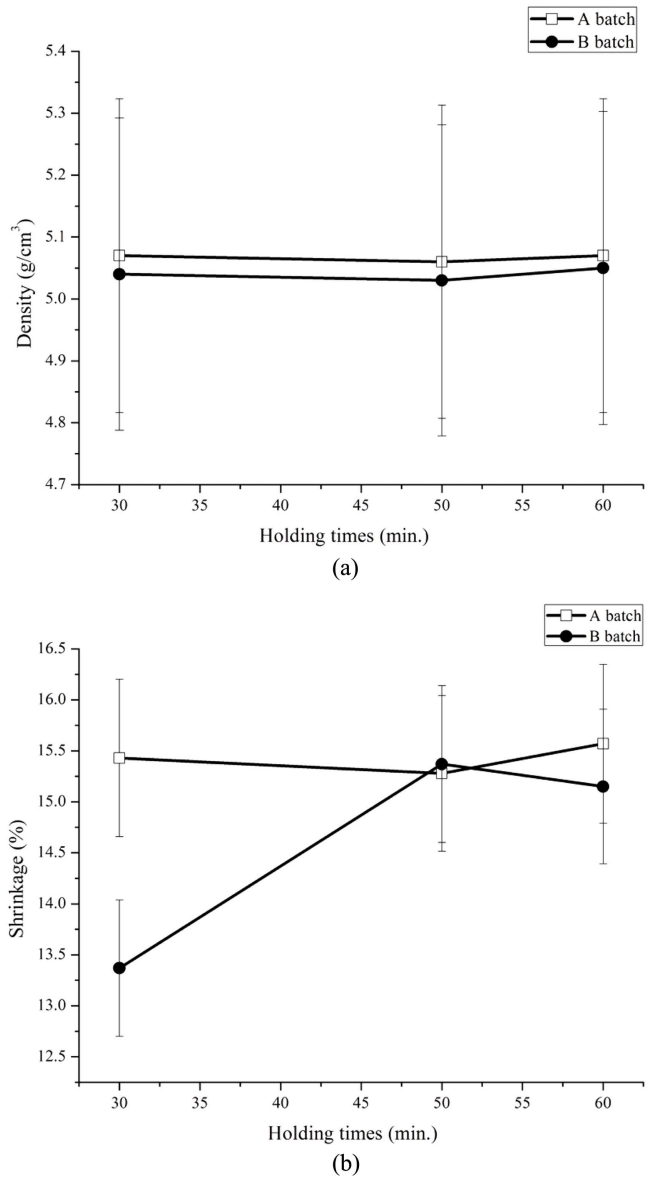

Fig. 2. (a) Density and (b) Shrinkage of (0.6)MZF-(0.4)BST ceramics under two stage sintering conditions.

composite materials [18]. The densification and percentage of shrinkage of ceramics sintered at various sintering condition are given in Fig. 2. It is observed that at a density of about 5.03-5.07 g/cm^3 the percentage of shrinkage values is between 13.37-15.57. The densification values are compatible to percentage of shrinkage values and tend to increase with lower sintering temperature of T_2. The high density of ceramics were achieved using holding times of T_1 for 60 min and sintering temperature of T_2 at 900 ºC with holding time for 5 h. It was found that (0.6)MZF-(0.4)BST ceramic samples prepared under two stage sintering had higher density values than when using conventional sintering reported by Rittidech *et al.* [8]. The average crystal size and lattice strain were calculated using the Williamson-Hall method [19]. MZF planes with (220), (311), (400) and BST planes with (110), (111), (002) were selected to calculation. The crystal sizes and lattice strain were obtained from average values of bulk composite ceramics shown in Table 1. The average crystal sizes and lattice strain of all samples were observed to be in the ranges of 53.87-54.68 nm and 1.30×10^{-3}-3.52×10^{-3}, respectively. Full pattern matching refinement of XRD patterns was performed using the TOPAS program based on the Rietveld method to obtain more detailed information on crystallographic spectra of (0.6)MZF-(0.4)BST and selected samples with holding times of T_1 for 60 min and sintering temperature of T_2 at 900 ºC holding time for 5 h are shown as the XRD refinement pattern in Fig. 3. The fitted patterns are in good agreement with the respective experiment data, denoted by R_p, R_{wp} and GOF factors listed in Table 1. The lattice parameter of the MZF cubic spinel is showed to be in the range of 8.414-8.416 Å, while the BST tetragonal phase is obtained tetragonality (c/a) in range of 1.00-1.004 Å. For higher values of T_2 sintering, an slight increase in crystal size and lattice strain values was obtained, which may be attributed to variation in the

Table 1. Rietveld refined structural parameters, profile R-factors, percentage of fraction phases, lattice strain and crystallize size of (0.6)MZF-(0.4)BST ceramics under two stage sintering conditions.

Sample	R-factor (%)			Lattice parameter of MZF (Å)	Percentage structure of MZF (%)	Lattice parameter of BST (Å)			Percentage structure of BST (%)	Lattice strain	Crystallite size (nm)
	Rp	Rwp	GOF			a	c	c/a			
A1	14.72	19.05	1.18	8.415(6)	57.34	3.976(9)	3.990(9)	1.004	42.23	1.30×10^{-3}	51.00
A2	12.76	16.34	1.33	8.416(9)	56.05	3.979(1)	3.981(9)	1.001	42.01	1.68×10^{-3}	51.34
A3	12.57	16.09	1.22	8.414(8)	56.88	3.978(0)	3.988(4)	1.003	41.68	2.42×10^{-3}	53.72
B1	12.59	16.02	1.40	8.415(4)	46.30	3.979(1)	3.980(8)	1.001	40.72	3.42×10^{-3}	54.25
B2	15.11	19.31	1.13	8.415(5)	44.99	3.981(5)	3.982(9)	1.000	41.57	3.52×10^{-3}	54.68
B3	15.18	19.20	1.29	8.415(7)	43.09	3.972(7)	3.989(2)	1.004	40.89	2.43×10^{-3}	53.87

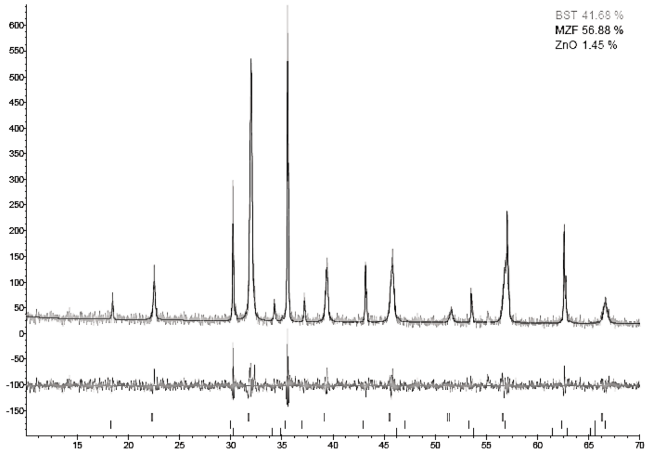

Fig. 3. Rietveld refinement of (0.6)MZF-(0.4)BST ceramics under two stage sintering conditions of T_1 at 1350 °C for 60 min and T_2 at 900 °C for 5 h.

lattice parameter.

SEM micrographs of (0.6)MZF-(0.4)BST sample (A3) are shown in the Fig. 4. It be observed that the combination of two phases between the ferroelectric (BST) and ferrite (MZF) phase, had a spherical grain shape with BST and an irregular grain shape with MZF, (Fig. 4, arrow). This result was confirmed using EDX analysis as shown in Fig. 5. Corresponding EDX analysis and chemical compositions for (0.6)MZF-(0.4)BST ceramics with different two stage sintering condition are revealed. It is seen that the composition (at%) of Zn decreased when using the second step sintering (T_2) at 1100 °C, supporting the presence of decreasing in densification results. The dielectric constant (ε_r) was measured as function of frequency for (0.6)MZF-(0.4)BST with various two stage sintering conditions as shown in Fig. 6. The dielectric constant decreased with increase in frequency and remain constant at higher frequencies. The high dielectric constant observed at lower frequencies is not intrinsic, but rather associated with heterogeneous conduction in multiphase structure of composite [20]. The dielectric constant values of (0.6)MZF-(0.4)BST ceramics with different two stage sintering conditions were measured at 25 °C as between 4.8×10^3 and 1.5×10^4 and the dense ceramic causes an increase in the dielectric values. The magnetic properties of the prepared samples have been determined at room temperature using a vibrating sample magnetometer (VSM) in an applied field ranging from −10 to +10 kOe. The hysteresis curves showing the variation of magnetization (M_s, emu/g) as a function of applied magnetic field (H, Oe) were plotted for (0.6)MZF-(0.4)BST ceramics sintered using various two stage sintering condition are shown in Fig. 7. The magnetic properties

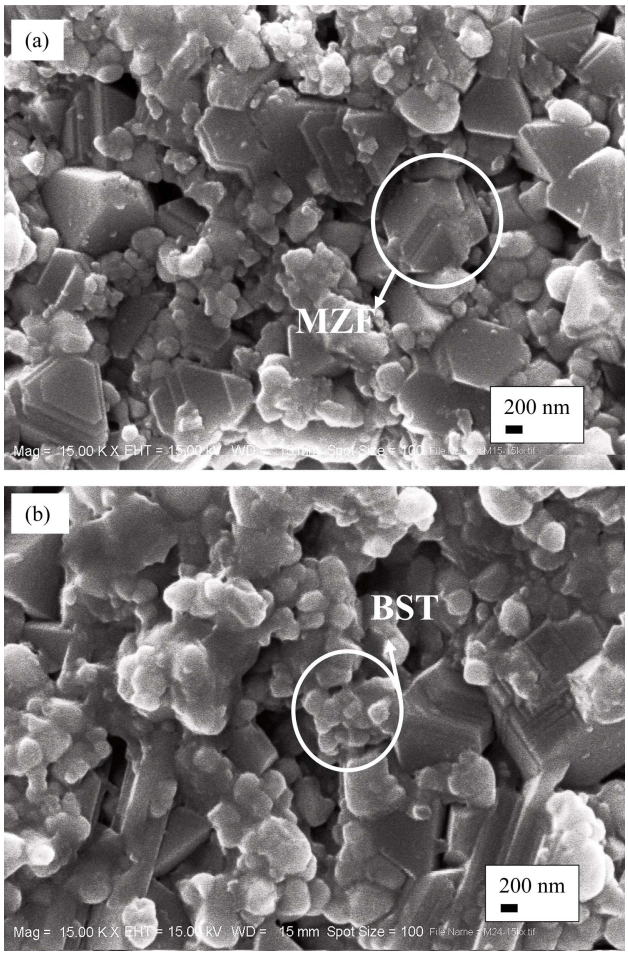

Fig. 4. SEM micrograph of (0.6)MZF-(0.4)BST ceramics under two stage sintering.

values such as saturation magnetization (M_s), remanent magnetization (M_r), the ratio of M_r/M_s or squareness factor and coercive force (H_c) are reported in Table 2. It is observed that sample from A batch showed higher M_r and H_c values than B batch but not clearly different for M_s values. (0.6)MZF-(0.4)BST ceramics from B batch were used sintering temperature of T_2 higher than A batch, which at higher temperature of T_2 cause ZnO phase loss, an important component of MZF ferrite phase, supporting

Table 2. Magnetic parameters of (0.6)MZF-(0.4)BST ceramics under two stage sintering conditions.

Sample	M_r (emu/g)	M_s (emu/g)	H_c (Oe)	M_r/M_s
A1	2.208	34.02	33.29	0.065
A2	2.711	32.75	34.41	0.083
A3	2.525	33.75	34.97	0.075
B1	1.528	34.82	21.92	0.044
B2	1.605	33.66	21.91	0.048
B3	1.853	34.26	26.10	0.054

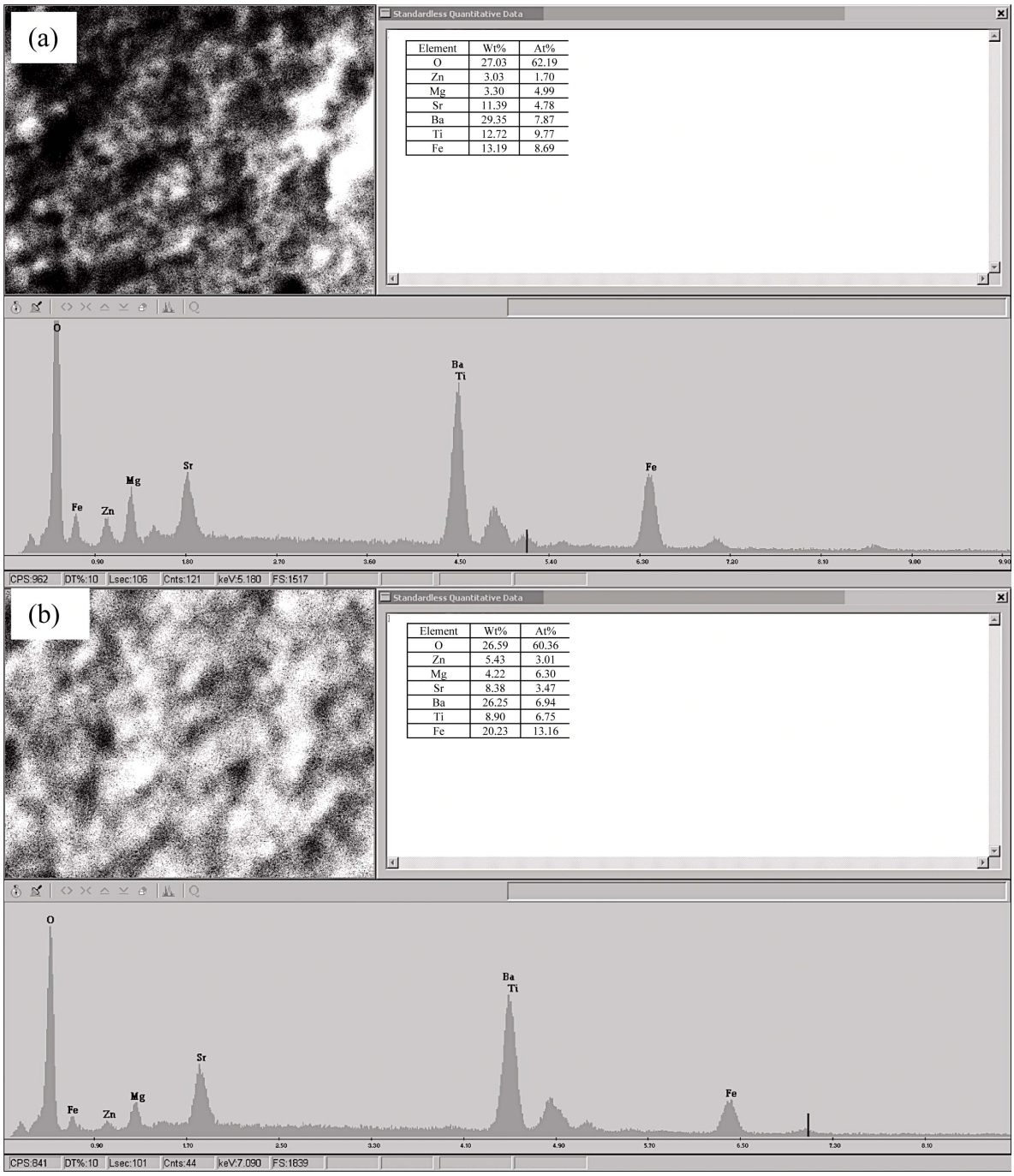

Fig. 5. EDX spectra of (0.6)MZF-(0.4)BST ceramics under two stage sintering conditions of T_1 at 1350 °C and (a) T_2 at 900 °C for 5 h, (b) 1100 °C for 5 h.

the densification and EDX results. It is found that on decreasing MZF ferrite phase structure fraction obtained from XRD refinement result (in Table 1) remanent magnetization (M_r), squareness factor and coercive force (H_c) decreases as presence of magnetic field. Although the higher sintering temperature of T_2 affects the evaporation of ZnO from MZF ferrite phase, it does not significantly influence the crystallize size and grain size of (0.6)MZF-(0.4)BST ceramics. This result indicates that the saturation magnetization (M_s) has a relation to the specific surface area, which increases as the grain size decreases, in agreement with other studies as Li *et al*. [10], Pandey *et al*. [21], and Gao *et al*. [22]. Therefor the saturation magnetization (M_s) of two batch showed similar behavior

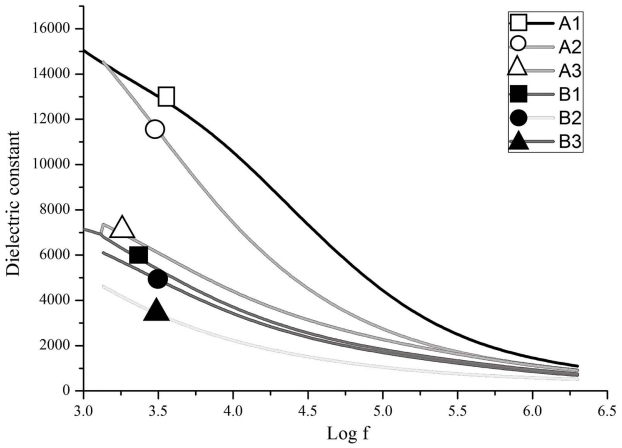

Fig. 6. Frequency dependences of dielectrics properties of (0.6)MZF-(0.4)BST ceramics under two stage sintering conditions.

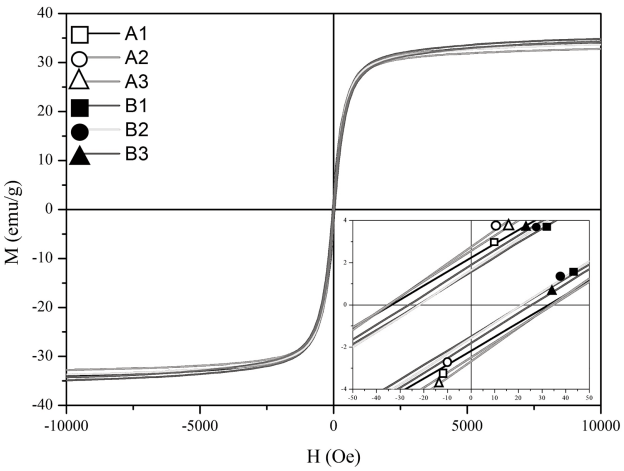

Fig. 7. M-H curves of (0.6)MZF-(0.4)BST ceramics under two stage sintering conditions.

due to the same molar ratio in composite materials. The result shows the dependence of dense ceramics on M_r and H_c values, which are obtained from the optimal short holding times of T_1 and lower sintering temperature of T_2 for long holding times. Moreover, it has been reported in the literature [15] that magnetic properties decrease probably due to the ZnO secondary phase consistent with XRD patterns results. The squareness factor which is often referred as reduced magnetization whose value lies between 0 and 1 and make the material for use in memory devices [23]. When the values of squareness factor are greater than or equal to 0.5, material reveals single magnetic domain while for values lower than 0.5 has a multi domain structure [24]. In this research the squareness factor lies values were obtained from 0.044 to 0.083, therefor the prepared composites are very useful in memory device applications.

Finally, the optimal two stage sintering conditions is established good electrical properties and magnetic properties and it can be found the first step sintering of T_1 at 1350 ºC using holding times between 50-60 min and the second step sintering of T_2 at 900 ºC for 5 h.

4. Conclusions

(0.6)MZF-(0.4)BST ceramics composites containing ferrite and ferroelectric phase were prepared by conventional methods under two stage sintering. The XRD patterns of composites enabled phase identification of ferrite and ferroelectric phase. Ceramic morphology were exhibited different grain shapes between irregular (ferrite) and spherical (ferroelectric) shape. Good electrical and magnetic properties were obtained from dense ceramics with short holding times of T_1 and lower sintering temperature of T_2.

Acknowledgment

The present work has been supported by Mahasarakham University. The authors are thankful to Faculty of Science and Mahasarakham University, Thailand for financial support to present in IFAAP2018 Japan (A. Sutthapintu) and ICAE2019 Korea (A. Rittidech).

References

[1] L. Bin, W. Chunnqing, Z. Wei, H. Chunjin, F. Jingming, and W. Hong, Mater. Lett. 91 (2013).
[2] B. Mirza, P. Vladimir, P. Shashank, B. Amar, Advance in Condensed Metter Physics (2012).
[3] P. Chee-Sung and P. Shashank, Advance in Condensed Metter Physics (2012).
[4] A. S. Tatarenko and M. I. Bichurin, Advance in Condensed Metter Physics (2012).
[5] Z. Hong-fang, W. O. Siu, and L. W. C. Helen, Mater. Res. Bull. 44 (2009).
[6] C. Choodamani, G. P. Nagabhushana, S. Ashoka, P. B. Daruka, B. Rudraswamy, and G. T. Chandrappa, J. Alloys and Compd. 578 (2013).
[7] E. S. Roxana, E. C. Cristina, H. Nadejda, G. Carmen, M. T. Florin, and M. Liliana, Ceram. Int. 42 (2016).
[8] A. Rittidech and A. Suthapintu, Ferroelectric 458 (2014).
[9] D. E. Garcia, A. N. Klein, and D. Hotza, Reviews on Advanced Materials Science 30 (2012).
[10] L. Qiang, B. Shengxiang, H. Tao, A. Libo, J. Yulan, and L. Jie, J. Magn. **23**, (2018).
[11] A. Rittidech, N. Porkornwong, and A. Suthapintu, Ferroelectric 382 (2010).

[12] R. B. Mohamad, G. Raziyeh, and L. Jae-Shin, Ceram. Int. 41 (2015).
[13] I. W. Chen and X. H. Wang, Nature 404 (2000).
[14] W. Siwei, Z. Lei, Z. Lingling, B. Kyle, and C. Fanglin, Electrochimica Acta 87 (2013).
[15] C. Choodamani, G. P. Nagabhushana, S. Askhoka, P. B. Duruka, and B. Rudraswamy, J. Alloys Compd. 578 (2013).
[16] Y. R. R. Pamela, A. C. H. Dora, C. E. B. José, M. A. R. José, J. S. F. Héctor, J. T. Argentina, E. D. L. P. Laura, M. N. Juan, and F. H. L. Gilberto, Magn. Magn. Mater. 427 (2017).
[17] G. Zhengang, P. Liqing, B. Chong, Q. Hongmei, Z. Xuedan, Y. Lihong, and M. R. Yasir, Magn. Magn. Mater. 325 (2013).
[18] T. M. D. Cao, H. T. T. Nhu, H. T. Kieu, T. Thi, C. T. Vinh, T. L. N. Bao, H. L. Van, A. D. Phuong, T. D. Anh, J. Heongkyu, and T. P. Bach, J. Magn. **20**, (2015).
[19] V. A. Jagadeesha, A. V. Anupama, K. C. Harish, R. Kumar, H. M. Somashekarrappa, M. Mallappa, B. Rudsawamy, and B. Sahoo, Ceram. Int. 246 (2017).
[20] K. Animesh, C. Upadhyay, and H. C. Verma, Phys. Lett. A 311 (2013).
[21] P. Rabichandra, K. P. Lagen, K. Sunil, and K. Manoranjan, J. Alloys Compd. 762 (2018).
[22] G. Rongli, Z. Qingmei, X. Zhiyi, W. Zhenhua, C. Gang, and D. Xiaoling, Composites Part B 166 (2019).
[23] D. Suita, H. Ashima, K. Satish, and M. Meena, J. Alloys Compd. 806 (2019).
[24] S. G. C. Fonsecaa, L. S. Neivab, M. A. R. Bonifacioc, P. R. C. Santosa, U. C. Silvad, and J. B. L. Oliveiraa, Mater. Res. 21 (2018).